

FC-05-1072 (Research Paper)

PRODUCTION OF HYDROGEN WITH LOW CARBON MONOXIDE FORMATION VIA CATALYTIC STEAM REFORMING OF METHANOL

SANJAY PATEL, K.K. PANT*

Indian Institute of Technology-Delhi, Department of Chemical Engineering,

Hauz-Khas, New Delhi-110016, India

Tel: +91-11-26596172, Fax: +91-11-26581120, Email: *kkpant@chemical.iitd.ac.in

Abstract

The production of hydrogen was investigated in a fixed bed tubular reactor via steam reforming of methanol (SRM) using CuO/ZnO/Al₂O₃ catalysts prepared by wet impregnation method and characterized by measuring surface area, pore volume, X-ray diffraction patterns and scanning electron microscopy photographs. The SRM was carried out at atmospheric pressure, temperature 493-573 K, steam to methanol molar ratio 1-1.8 and contact-time (W/F) 3-15 kg cat./(mol/s of methanol). Effects of reaction temperature, contact-time, steam to methanol molar ratio and zinc content of the catalyst on methanol conversion, selectivity and product yields was evaluated. The addition of zinc enhanced the methanol conversion and hydrogen production. The excess steam promoted the methanol conversion and suppressed the carbon monoxide formation. Different strategies have been mentioned to minimize the carbon monoxide formation for the steam reforming of methanol to produce PEM fuel cell grade hydrogen. Optimum operating conditions with appropriate composition of catalyst has been investigated to produce more selective hydrogen with minimum carbon monoxide. The experimental results were fitted well with the kinetic model available in literature.

Keywords: Hydrogen production; CO formation; CuO/ZnO/Al₂O₃; S/M molar ratio.

Introduction

Globally efforts are currently under way to minimize the emissions of NO_x, SO_x, hydrocarbons, CO and CO₂. Hydrogen is considered as a best fuel because of no emission of pollutants and high fuel density and also offers high efficiency when used in polymer electrolyte membrane (PEM) fuel cells. But the problem associated with hydrogen is the storage and transportation of it for the end use that is due to its high specific volume and undeveloped infrastructure for the transportation [1,2]. To overcome this hydrogen can be

produced as and when required from liquid organics like methanol, ethanol etc. Methanol is a promising hydrogen source due to several reasons like high hydrogen production yield can be obtained, can be converted at relatively low temperature, no sulphur and nitrogen compounds present, high hydrogen to carbon ratio (4:1) and no soot formation [3-5]. The best method to convert methanol into hydrogen rich stream may be a steam reforming of methanol process [2-4, 6-8]. Hydrogen produced by SRM process can be used as an energy source for stationary applications via fuel cell, especially in remote area. It can also be used in mobile carriers to prevent the emission of NO_x, SO_x and hydrocarbons with CO₂ formation reduction by more than 50% compared to internal combustion engine that uses gasoline as a fuel. The major problem with steam reforming of methanol is formation of CO that is harmful to the Pt anode of PEM fuel cell even if it presents in concentration of 20 ppm. Therefore in the preset study efforts have been made to reduce the CO formation by investigating appropriate catalyst and operating conditions for a steam reforming of methanol process. A series of CuO/ZnO/Al₂O₃ catalysts were prepared by varying Cu and Zn weight percent using wet impregnation method to maximize hydrogen yield and to suppress CO formation at a much lower concentration than it is at thermodynamic equilibrium for the SRM process. The different strategies have also been investigated to minimize the CO formation. Kinetic parameters of kinetic model available in the literature were estimated using our experimental results followed by validation of kinetic model with experimental data.

Experimental

Catalyst Preparation. CuO/ZnO/Al₂O₃ catalysts were prepared by wet impregnation method. The catalyst properties are given in Table 1. In all the catalysts the copper was the active phase, zinc oxide was used to improve the dispersion of copper and its reducibility while the alumina was used to

improve the surface area and to lower the sintering of the catalyst. The alumina pellets were dipped in the excess solution of copper nitrate 3-hydrate ($\text{Cu}(\text{NO}_3)_3 \cdot 3\text{H}_2\text{O}$) and zinc nitrate 6-hydrate ($\text{Zn}(\text{NO}_3)_6 \cdot 6\text{H}_2\text{O}$) (Merck, Germany) for 4 h with stirring. The advantage of providing excess solution was that precursors became distributed uniformly throughout the pores. Excess water was removed in the rotary vacuum evaporation unit followed by drying of precursors overnight at 383 K. Calcination in the presence of air at 603 K for 5 h was carried out to get metal oxides. Calcined catalysts were crushed and sieved to a particle size of 20-25 mesh size prior to use for the SRM reaction. The pre-reduction of catalysts was carried out in situ using 10% hydrogen and 90% nitrogen mixture stream with a heating rate of 5 K/min and dwelling at 487 K for 2 h.

Catalytic Activity for Steam Reforming of Methanol.

Preliminary experiments were carried out with varying particle size of the catalyst and the weight hourly space velocity to select the range of operating conditions where mass transfer resistances could be neglected. Catalyst particle size varied from 0.4-1 mm. The results are depicted in Fig. 1. For the particle size smaller than 0.6 mm methanol conversion was almost constant, therefore average particle size 0.6 mm corresponds to 20/25 mesh was used throughout all the experiments to minimize the intraparticle diffusion.

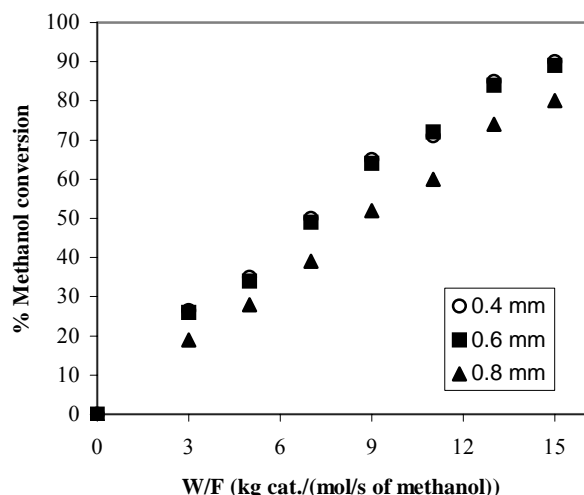


Fig. 1 Effect of particle size on methanol conversion

The catalyst particles were diluted in the Pyrex quartz beads of same size to achieve the isothermal conditions. Further to avoid the thermal gradients and mass transfer limitations, high weight hourly space velocity (WHSV) between 7 and 38 1/h was maintained. The back mixing and channeling was eliminated by providing catalyst bed height to catalyst particle size ratio, $L/D_p \geq 50$ and that of internal diameter of reactor to catalyst particle size, $D/D_p \geq 30$ respectively based on literature [9,10].

Catalysts performance was evaluated in a fixed-bed stainless steel reactor (19 mm i.d.) with 1-3 gm catalyst loading. Methanol steam reforming reaction was carried out at atmospheric pressure by placing the reactor in an insulated electric furnace consisting of two heating zones with two PID temperature controllers. Operating temperature and contact-time (W/F) varied from 493-593 K and 3-15 kg cat./mol of methanol respectively. A thermocouple was placed at the center of catalyst bed to monitor catalyst bed temperature. Liquid methanol and water were supplied separately to the preheater using peristaltic pumps. The preheater was maintained at 463 K, where reactants got vaporized and mixed. Vaporized reactants fed to the reactor for steam reforming of methanol reaction. The products and unconverted reactants were passed through the condenser and liquid-gas separator followed by sampling ports. Reaction products were analyzed by Nucon-5700 Gas chromatograph, equipped with thermal conductivity detector having carbosphere column for gaseous product concentration measurement and flame ionization detector with silica-alumina fused capillary column for unconverted liquid reactants.

Results and Discussion

Catalysts Characterization. Surface area, pore volume and pore size of different $\text{CuO}/\text{ZnO}/\text{Al}_2\text{O}_3$ catalysts are listed in Table 1. BET surface area varied from 128-158 m^2/g . It can be seen that an increase in CuO loading onto catalysts resulted in a decrease in surface area due to porous structure of the support occupied by catalyst molecules.

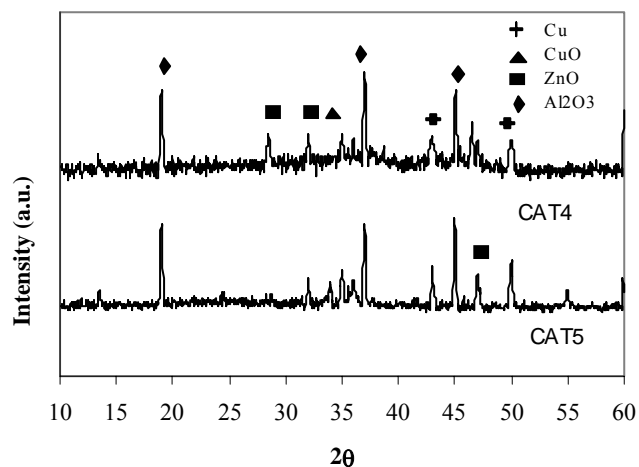
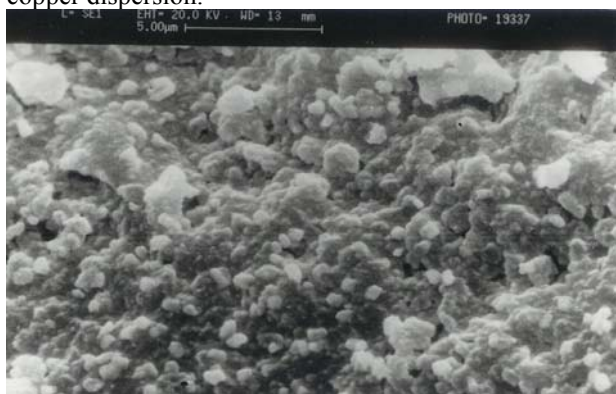


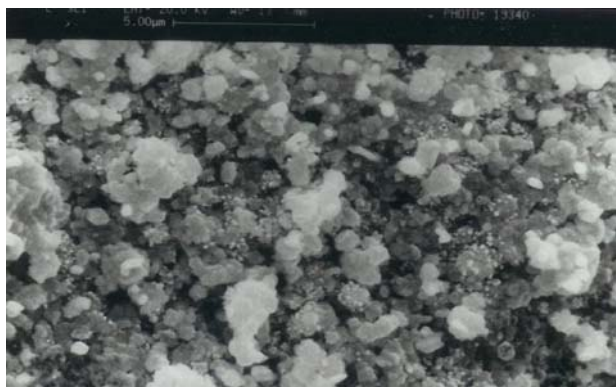
Fig. 2. X-ray diffraction patterns of reduced fresh catalysts.

X-ray diffraction patterns (Fig. 2) revealed that on the reduction of catalyst copper oxide reduced to the copper while zinc oxide remained in oxide form only. As per Scherrer formula $\psi = (\varphi * \lambda) / (\beta * \cos\theta)$; where, ψ is a measure of the dimension of particle in diffraction perpendicular to the reflecting plane, λ is the X-ray wavelength, β is peak width and $\varphi=1$ a constant; particle size is inversely proportional to the

peak width at constant θ and λ . The peak width of Cu phase for CAT4 is wider than that for CAT5, indicating that particle size of Cu in CAT4 is smaller, and smaller the crystallites better the copper dispersion.



(a)



(b)

Fig. 3. SEM photographs of CAT4 (a) fresh catalyst (b) spent catalyst

The SEM photographs of fresh and spent catalysts are shown in Fig. 3 (a) and (b) respectively. The average grain size of spent catalyst, used for 60 h run-time, was $1\pm 0.05 \mu\text{m}$, which was marginally larger than the fresh catalyst ($0.9\pm 0.05\mu\text{m}$). There was no significant change in the morphology and surface structure of CAT4 observed.

Comparison of Catalytic Activity. The methanol conversion for different catalysts as a function of contact-time at 513 K is shown in Fig. 4. The maximum conversion was obtained using CAT4 with composition Cu/Zn/Al₂O₃:10/5/85 wt% and lowest was with CAT1 containing 15 wt% copper with no zinc oxide, which indicates that the promoter zinc enhances the catalytic activity of SRM. CAT5 with same copper amount as CAT4 but with higher zinc loading showed lower activity. In conjunction with Table 1 and above discussion, the optimum Cu/Zn wt% ratio was the 2. The highest activity of CAT4 was due to its high surface area and better copper dispersion obtained by optimum loading of copper and zinc, and also CAT4 prepared by wet impregnation

required less amount of copper and zinc compared to amounts used in co-precipitation method [6, 11-14].

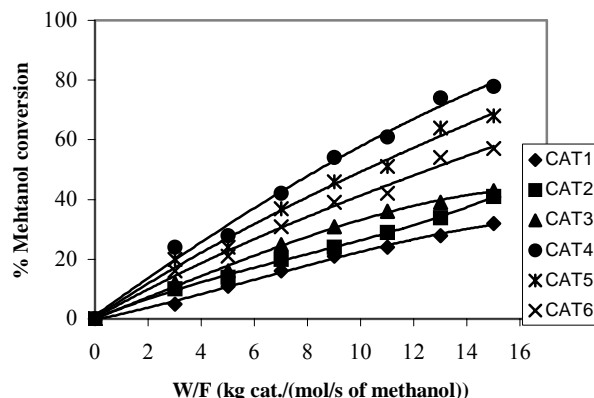


Fig. 4. Effect of contact-time on methanol conversion for different CuO/ZnO/Al₂O₃ catalysts. (T=513 K, S/M=1.4 molar, P=1 atm)

Effect of Contact-time. The effect of contact-time was investigated by varying W/F (weight of catalyst/molar flow rate of methanol) ratio from 3-15 kg cat./mol of methanol). Methanol conversion as a function of contact-time for the catalyst CAT4 (Cu/Zn/Al₂O₃:10/5/85) at different reaction temperatures for steam reforming of methanol is presented in the Fig. 5.

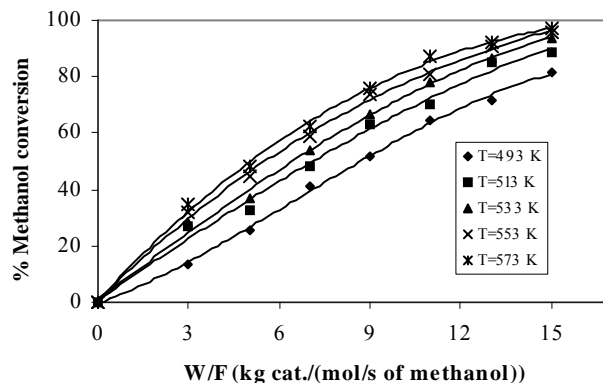


Fig. 5. Effect of contact-time on methanol conversion at different temperatures. (catalyst cat4, S/M =1.4 molar, P=1 atm)

Methanol conversion increased rapidly with contact-time at all the temperatures. As W/F increased more active sites of catalysts available to the reactants to give rise in methanol conversion. Methanol conversion and products selectivity (mols of product per mol of methanol reacted) is shown in Fig. 6.

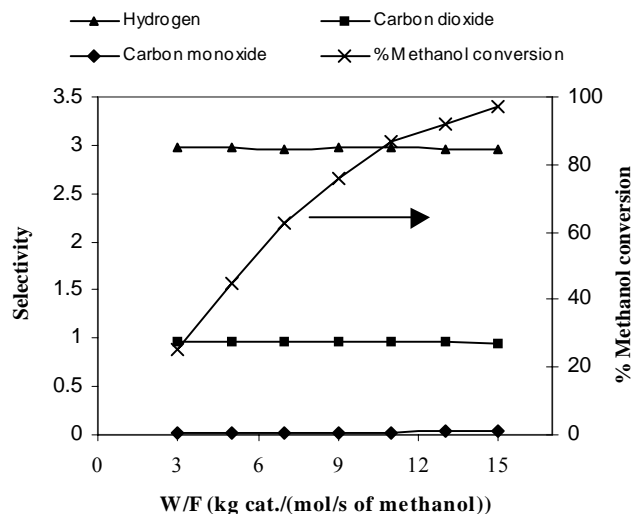


Fig. 6. Effect of contact-time on methanol conversion and product selectivity.
(catalyst CAT4, T=573 K, S/M=1.4 molar, P=1 atm)

The CO selectivity increased from 0.002 to 0.022 as W/F increased from 5 to 15 kg cat./(mol/s of methanol) due to increase in rate of reverse water gas shift reaction (Eq. 3) that can also be concluded by observing the marginal decrease in H₂ and CO₂ selectivity at higher conversion of methanol as shown in Table 2.

Table 2. Effect of contact time on product rates and selectivity (T=573 K, P=1 atm)

W/F*	X	H ₂	CO ₂	CO	CO	H ₂	CO ₂	CO
	%	mmol s ⁻¹ kg ⁻¹	mmol s ⁻¹ kg ⁻¹	mmol s ⁻¹ kg ⁻¹	mol%	Selectivity, mol/mol	Selectivity, mol/mol	Selectivity, mol/mol
3	34.8	349	116	0.29	0.062	2.99	0.99	0.002
5	48.2	290	96	0.41	0.106	2.99	0.99	0.004
7	62.7	268	89	0.55	0.153	2.99	0.99	0.006
9	75.7	252	83	0.67	0.198	2.99	0.99	0.008
11	87.0	236	78	0.80	0.254	2.98	0.98	0.010
13	91.9	211	69	1.23	0.436	2.98	0.98	0.017
15	97.0	192	62	3.16	1.223	2.97	0.97	0.022

* kg cat./(mol/s of methanol))

The yield (mols of product per mol of methanol fed to reactor) of H₂, CO₂ and CO has shown increasing trend as a function of W/F because of increase in methanol conversion.

Effect of Temperature. Steam reforming of methanol initiates at about 423 K and approximately 100% conversion of methanol can be obtained at the temperature greater than 473 K under specific reaction conditions. The conversion increases with temperature because of reforming and decomposition reactions; both are endothermic; as a result, a small increase in temperature resulted in a significant increase in methanol

conversion. The formic acid did not form as an intermediate, which is in agreement with the observations of Breen and Ross [15].

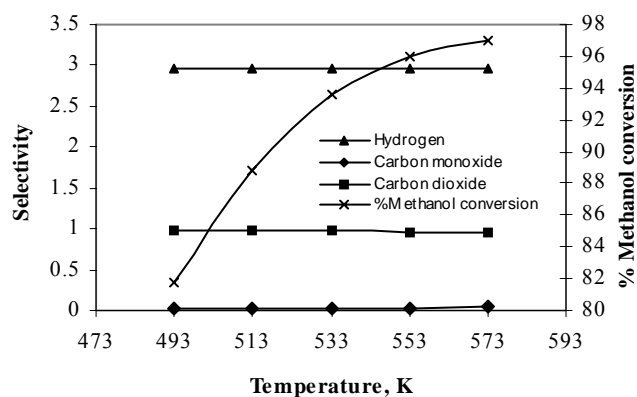


Fig. 7. Effect of temperature on methanol conversion and selectivity.
(catalyst CAT4, W/F=15 kg cat./(mol/s of methanol), S/M=1.4 molar, P=1 atm)

The yield of products increased with the temperature. On the other hand selectivity of H₂ and CO₂ decreased while that of CO increased; as shown in Fig. 7; indicating that reverse water gas shift reaction accelerated. The product formation rate as well as selectivities at different reaction temperatures is shown in Table 3.

Table 3. Effect of temperature on product rates and selectivity (W/F=15 kg_{cat} s mol⁻¹, P=1 atm)

T	X	H ₂	CO ₂	CO	CO	H ₂	CO ₂	CO
K	%	mmol s ⁻¹ kg ⁻¹	mmol s ⁻¹ kg ⁻¹	mmol s ⁻¹ kg ⁻¹	mol%	Selectivity, mol/mol	Selectivity, mol/mol	Selectivity, mol/mol
493	81.8	163	53	1.55	0.708	2.97	0.97	0.028
513	88.8	177	58	1.72	0.723	2.97	0.97	0.028
533	93.6	187	61	1.85	0.738	2.97	0.97	0.029
553	96.0	191	62	2.37	0.924	2.96	0.96	0.036
573	97.0	192	62	3.16	1.223	2.95	0.95	0.048

Effect of Steam to Methanol Molar Ratio. The excess steam promoted methanol conversion and reduced CO formation by shifting the equilibrium of reverse WGS reaction (Eq. 3) to left. The effect of steam to methanol molar ratio on activity of CAT4 catalyst at reaction temperature 553 K is shown in Fig. 8. Methanol conversion increased appreciably as steam to methanol molar ratio was increased from 1.0-1.5 and beyond which increase in conversion was gradual. CO concentration at S/M 1.0 was 0.24 mol% and it reduced to 0.08 mol% at S/M 1.8.

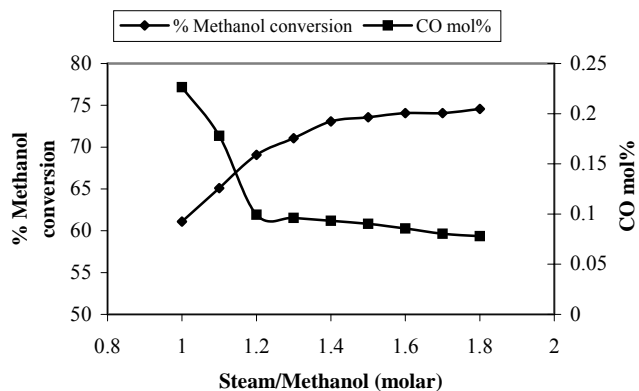


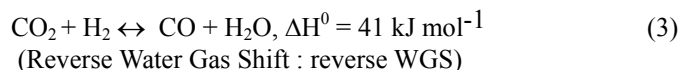
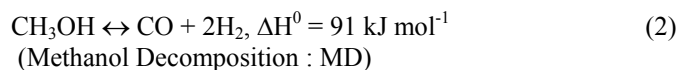
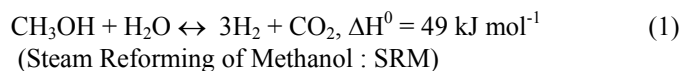
Fig. 8. Effect of S/M molar ratio on methanol conversion and carbon monoxide formation. (catalyst CAT4, T=553 K, W/F=9 kg cat./(mol/s of methanol), P=1 atm)

Results indicate that high S/M molar ratio is favorable for the methanol conversion and for reducing the CO concentration in product stream. The optimum S/M molar ratio can be recommended as 1.4-1.5 because further increase of S/M molar ratio has negligible effect on CO formation; instead it increases reactor load and diluting the product stream. Our results indicate that CO level is influenced by the temperature of reaction, degree of methanol conversion and steam to methanol molar ratio. Methyl formate was not detected in the range of experiments. The results agreed with the reaction scheme proposed by Agrell et al. [16] who considered the CO formation via reverse WGS (Eq. 2) reaction as a secondary product. There was no CO formation observed for the temperature range 423-453 K that suggests CO formed at higher temperature via reverse WGS reaction as a secondary product. CO concentration at all the reaction temperatures 473-573 K was much less than the equilibrium values based on thermodynamics for water gas shift reaction, which revealed that CO₂ can not be formed from CO by WGS reaction. These confirmed that the SRM (Eq. 1) and reverse WGS (Eq. 3) reactions play major role in SRM process with very less contribution of methanol decomposition reaction (Eq. 2).

CO clean-up. In present study CO content was found in the range from 0.06-1.2 mol%, which is lower than the reported by others using CuO/ZnO/Al₂O₃ [6, 11-14]. However, CO in levels exceeding a 20 ppm poisons the PEM fuel cell by blocking the active sites of the platinum-based anode electrocatalyst, thus hampering the fuel cell performance. Therefore, CO has to be removed for the successful operation of the fuel cell. The choice of clean-up technology affects both the design and the overall efficiency of the fuel cell system. Efficient suppression of CO formation in the reforming reactor reduces the load, size and cost of the CO clean-up unit and also improves the overall efficiency of the system. Possible technologies for CO abatement include preferential oxidation (PROX), water gas shift reaction followed by preferential

oxidation, reduction (methanation), adsorption or the use of palladium membranes. Preferential oxidation (PROX), involves the oxidation of CO with O₂ or air [17,18]. The technological challenge lies in the oxidation of CO in presence of excess H₂, without loss of H₂ through direct oxidation. Present practice feeds twice the stoichiometric amount of oxygen necessary to oxidize the CO to the oxidation system. Major efforts have been focused on alumina-supported platinum catalysts for PROX. This process is suitable when CO concentration is low (about 1-2 mol%). The high-temperature and low temperature shift reactions are used when CO concentration is higher, which also requires further purification to obtain PEM fuel cell grade hydrogen. Another method is the methanation in which CO is converted into methane by reaction with H₂ [19]. Each converted molecule of CO consumes three H₂ molecules; the system suffers a substantial H₂ loss. Since the CO produced in present study is quite low the PROX is a suitable method for removing the CO from the hydrogen rich stream to use it as a feed for the PEM fuel cell. Geissler et al. [20] reported that the addition of CO clean-up unit in reformat based PEM fuel cell system reduces the over all efficiency only by 1%.

Kinetics Study. The main reactions involved during SRM process over CuO/ZnO/Al₂O₃ catalysts are as following.



Jiang et al. [11,12] explicitly defined a set of elementary surface reactions, to obtain a mechanistic Langmuir-Hinshelwood rate expression. They obtained the following rate expression:

$$r_R = \frac{k_{\text{CH}_3\text{O}} \left(\frac{K_{\text{CH}_3\text{OH}}}{K_{\text{H}_2}} \right)^{1/2} \left(\frac{p_{\text{CH}_3\text{OH}}}{p_{\text{H}_2}} \right)^{1/2}}{\left(1 + \left(\frac{K_{\text{CH}_3\text{OH}}}{K_{\text{H}_2}} \right)^{1/2} \left(\frac{p_{\text{CH}_3\text{OH}}}{p_{\text{H}_2}} \right)^{1/2} + \frac{K_{\text{H}_2}^{1/2}}{p_{\text{H}_2}^{1/2}} \right)^2} (C_S T)^2 \quad (4)$$

Where the only adsorption of methanol and the adsorption of hydrogen were found to have statistically significant effects on the rate of reaction. The kinetic expression developed by Jiang et al. [12] predicts the rate of disappearance of methanol and the rate of formation of CO₂ only. For the PEM fuel cell applications, where very low levels of CO contamination severely poison the anode electrocatalyst, the decomposition reaction and the WGS reaction must be taken into account. Peppley et al. [13,14] developed the surface mechanisms for SRM over CuO/ZnO/Al₂O₃ catalysts, which account for all

three of the possible overall reactions: methanol and steam reacting directly to form H₂ and CO₂ (Eq. 1), methanol decomposition to H₂ and CO (Eq. 2) and the reverse water gas shift reaction (Eq. 3). The key features of the mechanism are: (i) that hydrogen adsorption does not compete for the active sites which the oxygen-containing species adsorb on, (ii) there are separate active sites for the decomposition reaction distinct from the active sites for the methanol-steam reaction and the water gas shift reaction, (iii) the rate-determining step (RDS) for both the methanol-steam reaction and the methanol decomposition reaction is the dehydrogenation of adsorbed methoxy groups and (iv) the RDS for the water gas shift reaction is the formation of an intermediate formate species.

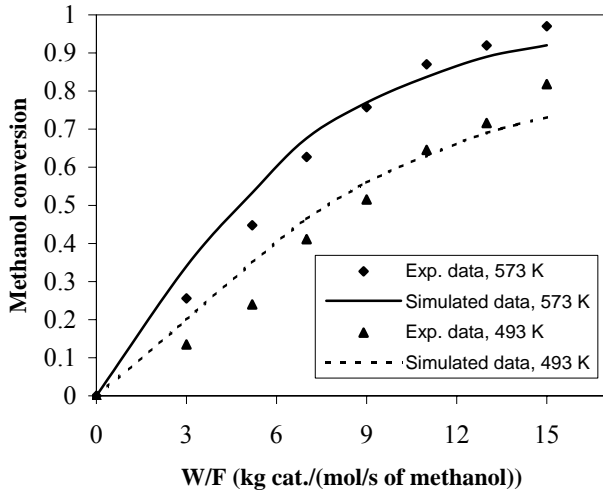


Fig. 9. Experimental and Model predicted methanol conversion as a function of contact-time. (P=1 atm, S/M Ratio =1.4 Molar)

A kinetic model was developed by Peppley et al. [14] based on an analysis of the surface mechanism.

$$r_R = \frac{k_R^* K_{CH_3O}^{(1)} \frac{p_{CH_3OH}}{p_{H_2}} \left(1 - \frac{p_{H_2}^3 p_{CO_2}}{K_R p_{CH_3OH} p_{H_2O}} \right) C_{S1}^T C_{S1a}^T}{\left(1 + K_{CH_3O}^{(1)} \frac{p_{CH_3OH}}{p_{H_2}} + K_{HCOO}^{(1)} p_{CO_2} p_{H_2}^{1/2} + K_{OH}^{(1)} \frac{p_{H_2O}}{p_{H_2}} \right) \left(1 + K_H^{(1a)} p_{H_2}^{1/2} \right)} \quad (5)$$

$$r_D = \frac{k_D^* K_{CH_3O}^{(2)} \frac{p_{CH_3OH}}{p_{H_2}} \left(1 - \frac{p_{H_2}^2 p_{CO}}{K_D p_{CH_3OH}} \right) C_{S2}^T C_{S2a}^T}{\left(1 + K_{CH_3O}^{(2)} \frac{p_{CH_3OH}}{p_{H_2}} + K_{OH}^{(2)} \frac{p_{H_2O}}{p_{H_2}} \right) \left(1 + K_H^{(2a)} p_{H_2}^{1/2} \right)} \quad (6)$$

$$r_W = \frac{k_W^* K_{OH}^{(1)} \frac{p_{CO} p_{H_2O}}{p_{H_2}^{1/2}} \left(1 - \frac{p_{H_2} p_{CO_2}}{K_W p_{CO} p_{H_2O}} \right) C_{S1}^T C_{S1}^T}{\left(1 + K_{CH_3O}^{(1)} \frac{p_{CH_3OH}}{p_{H_2}} + K_{HCOO}^{(1)} p_{CO_2} p_{H_2}^{1/2} + K_{OH}^{(1)} \frac{p_{H_2O}}{p_{H_2}} \right)} \quad (7)$$

In the present study, the kinetic model proposed by Peppley et al. [14] was used and compared with the experimental data.

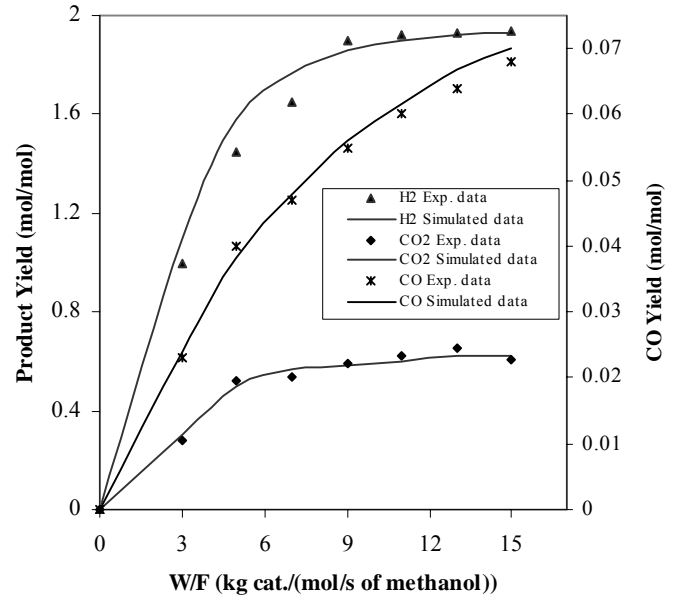


Fig. 10. Experimental and model predicted yield of H₂, CO₂ and CO at 553 K as a function of contact-time.

The parameters of kinetic model were estimated using our experimental data by non-linear regression. Comparison between experimental and model predicted methanol conversion at different temperatures as a function of contact-time is shown in Fig. 9. The experimental and model predicted product yields is also presented in Fig. 10, which closely match with the experimental data with regression coefficient R²=0.96

Nomenclature

C _{si} ^T	total surface concentration of site i mol/m ²
D	reactor inner diameter, mm
D _p	catalyst particle size, mm
L	catalyst bed height, mm
K _i	equilibrium constant of reaction i or adsorption coefficient for surface species i
k _i	rate constant for reaction i; units will be specific to the form of the rate expression

p_i	partial pressure of component i (atm)
r_i	rate of reaction of component i (mol/s m ²)
S_i	active site i in reaction mechanism

Greek symbols

ψ	measure of the dimension of particle in diffraction perpendicular to the reflecting plane
φ	constant=1
λ	X-ray wavelength
β	peak width of XRD
θ	diffraction angle

Subscripts

R	methanol steam reforming reaction
W	water gas shift reaction
D	decomposition reaction
1	active site 1 when on variable S
1a	active site 1a when on variable S
2	active site 2 when on variable S
2a	active site 2a when on variable S

Superscripts

(i)	species adsorbed on active site i where i is, 1, 1a, 2 or 2a
T	indicating total concentration of active sites

Acronyms

MD	methanol decomposition
PEM	polymer electrolyte membrane
PID	proportional integral derivative
PROX	preferential oxidation
RDS	rate determining step
SEM	scanning electron microscopy
S/M	steam to methanol molar ratio
SRM	steam reforming of methanol
W/F	weight of catalyst/molar flowrate of methanol
WGS	water gas shift
WHSV	weight hourly space velocity
XRD	X-ray diffraction

Conclusion

The catalyst CAT4 having composition Cu/Zn/Al₂O₃:10/5/85 wt% has been found effective for the production of hydrogen by steam reforming of methanol. The addition of ZnO enhances the Cu/Al₂O₃ catalyst activity for hydrogen production by increasing copper dispersion resulting due to smaller copper crystallite sizes. Methanol conversion increased with increasing temperature, contact-time and steam to methanol molar ratio, which maximized the hydrogen production. On the other hand CO formation increased with temperature and contact time while decreased as a function of steam to methanol ratio. The product distribution indicates that the carbon monoxide formed as a secondary product and its concentration was very low in the range 0.06-1.2 mol%. The hydrogen rich stream produced in present study can be used as a PEM fuel cell feed after preferential oxidation of the CO.

Experimental data fitted well with the kinetic model available in the literature.

References

- [1] Raimondi, F., Geissler, K., Wambach, J. and Wokaun, A., 2002, "Hydrogen production by methanol reforming: post-reaction characterisation of a Cu/ZnO/Al₂O₃ catalyst by XPS and TPD," *Appl. Sur. Sci.*, 189, pp. 59-71.
- [2] Lindstrom, A., Pettersson, L. J. and Menon, P. G., 2002, "Activity and characterization of Cu/Zn, Cu/Cr and Cu/Zr on γ -alumina for methanol reforming for fuel cell vehicles," *Appl. Catal.A*, 234, pp.111-125.
- [3] Ahmed, S., and Krumpelt, M., 2001, "Hydrogen from hydrocarbon fuels for fuel cells," *Inter. J. of Hydrogen Energy*, 26, pp. 291-301.
- [4] Kniep, B.L., Girgsdies, F. and Ressler, T., 2005, "Effect of precipitate aging on the microstructural characteristics of Cu/ZnO catalysts for methanol steam reforming," *J. Catal.*, 236, pp. 34-44.
- [5] Wiese, W., Emonts, B. and Peters. R., 1999, "Methanol reforming in a fuel cell drive system," *J. Power Sources*, 84, pp.187-193.
- [6] Durga, K.V., Subrahmanyam, M., Ratnamala, A., Venugopal, D., Srinivas, B., Sharma, M. V. P., Madhavendra, S. S., Bikshapathi, B., Venkateswarlu, K., Krishnudu, T., 2002, "Correlation of activity and stability of CuO/ZnO/Al₂O₃ methanol steam reforming catalysts with Cu/Zn composition obtained by SEM-EDAX analysis," *Catalysis Communication*, 3, pp. 417-424.
- [7] Suwa, Y., Ito, S., Kameoka, S., Tomishige, K. and Kunimori, K., 2004, "Comparative study between Zn-Pd/C and Pd/ZnO catalysts for steam reforming of methanol," *Appl. Catal.A*, 267, pp. 9-16.
- [8] Matter, P. H., Braden, D. J. and Ozkan, U. S., 2004, "Steam reforming of methanol to H₂ over nonreduced Zr-containing CuO/ZnO catalysts," *J. Catal.*, 223, pp. 340-351.
- [9] Idem, R.O. and Bakhshi, N.N., 1994, "Production of Hydrogen from Methanol. 1. Catalyst characterization studies," *Ind. Eng. Chem. Res.*, 33, pp. 2047-2058.
- [10] Froment, G.F. and Bischoff, K.B. 1990, "Chemical reactor analysis and design," 2nd ed., New York: Wiley; 1990.
- [11] Jiang, C.J., Trimm, D.L., Wainwright, M.S. and Cant, N.W., 1993, "Kinetic mechanism for the reaction between methanol and water over a Cu-ZnO-Al₂O₃ catalyst," *Appl. Catal.A*, 97, pp. 145-158.
- [12] Jiang, C.J., Trimm, D.L., Wainwright, M.S. and Cant, N.W., 1993, "Kinetic study of steam reforming of methanol over copper-based catalysts," *Appl. Catal.A*, 97, pp. 245-255.
- [13] Peppley, B.A., Amphlett, J.C., Kearns, L.M. and Mann, R.F., 1999, "Methanol-steam reforming on

- Cu/ZnO/Al₂O₃. Part 1: the reaction network,” Appl. Catal.A, 179, pp. 21-29.
- [14] Peppley, B.A., Amphlett, J.C., Kearns, L.M. and Mann, R.F., 1999, “Methanol–steam reforming on Cu/ZnO/Al₂O₃. Part 2. A comprehensive kinetic model,” Appl. Catal.A, 179, pp. 31-49.
- [15] Breen, J. P. and Ross, J. R. H., 1999, “Methanol reforming for fuel-cell applications: development of zirconia-containing Cu–Zn–Al catalysts,” Catal. Today, 51, pp. 521-533.
- [16] Agrell, J., Birgersson, H. and Boutonnet, M., 2002, “Steam reforming of methanol over a Cu/ZnO/Al₂O₃ catalyst: a kinetic analysis and strategies for suppression of CO formation ,” J. Power Sources, 106, pp. 249-257.
- [17]] Sekizawa, K., Yano, S., Eguchi, K. and Arai, H., 1998, “Selective removal of CO in methanol reformed gas over Cu-supported mixed metal oxides,” Appl. Catal.A, 169, pp. 291-297.
- [18] Dudfield, C. D., Chen, R. and Adcock, P. L., 2000, “Evaluation and modelling of a CO selective oxidation reactor for solid polymer fuel cell automotive applications,” J. Power Sources, 85, pp. 237-244.
- [19] Oshiro, H. , Nagaya, K., Mitani, K. and Tsuchiyama, S., 1996, Proceedings of Fuel Cell Seminar, Orlando, Florida, 1996, pp. 319-324.
- [20] Geissler, K., Newson, E., Vogel, F., Truong, T.B., Hottinger, P. and Wokaun, A., 2001, “Autothermal methanol reforming for hydrogen production in fuel cell Applications,” Phys. Chem. Chem. Phys., 3, pp. 289-293.

Table 1. Properties of catalysts

Catalysts	CAT1	CAT2	CAT3	CAT4	CAT5	CAT6
Cu/Zn/Al ₂ O ₃ , wt%	15/0/85	5/12/83	5/10/85	10/5/85	10/7/83	12/6/82
BET surface area, m ² /g	139	128	136	158	151	141
Pore volume, cm ³ /g	0.33	0.23	0.28	0.35	0.34	0.32
Avg. D _p , A ^o	68	52	54	64	61	59